Comparison of various methods to extract ringdown frequency from gravitational wave data --- Mockdata challenge of 5 methods

Hiroyuki Nakano, Tatsuya Narikawa, Ken-ichi Oohara, Kazuki Sakai, Hisa-aki Shinkai*, Hirotaka Takahashi, Takahiro Tanaka, Nami Uchikata, Shun Yamamoto, and Takahiro Yamamoto

*hisaaki.shinkai@oit.ac.jp

Outline & Summary

The ringdown part of gravitational waves in the final stage of merger of compact objects tells us the nature of strong gravity which can be used for testing the theories of gravity. The ringdown waveform, however, fades out in a very short time with a few cycles, and hence it is challenging for gravitational wave data analysis to extract the ringdown frequency and its damping time scale. We here propose to build up a suite of mock data of gravitational waves to compare the performance of various approaches developed to detect quasi-normal modes from a black hole. In this paper we present our initial results of comparisons of the following five methods;

(1a) plain matched filtering with ringdown part (MF-R) method,
(1b) matched filtering both merger and ringdown parts (MF-MR) method,
(2) Hilbert-Huang transformation (HHT) method,
(3) autoregressive modeling (AR) method, and
(4) neural network (NN) method.

More details:

https://gw-genesis.scphys.kyoto-u.ac.jp/ilias/goto_root_fold_669.html
http://www.oit.ac.jp/is/shinkai/mockdatachallenge/

Phys. Rev. D 99, 124032 (2019) [arXiv:1811.06443]

Motivation & Mockdata

Towards testing gravity theories ⇒ Ringdown-part extraction is a key

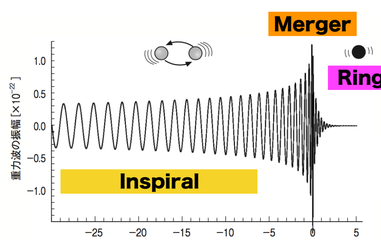

BH quasi-normal modes
⇦ BH perturbation theory
⇨ (*M, a*)
strongest gravity we can observe
⇨ test of gravity theories

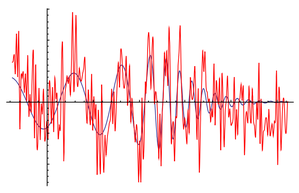

For *60M* BH of *a*=0.75,
frequency = 300 Hz
damping time scale = 3.7 ms

Mockdata preparation

SXS data + shifted ringdown injection + aLIGO noise
modified after t_merger (set A) 60 set
modified before/after t_merger (set B) 60 set

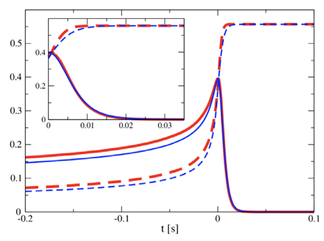

FIG. 1. Examples of sets A and B. (Inset) The ringdown part. Here, set A [(red) thick] with SXS:BBH:0174 and set B [(blue) thin] with SXS:BBH:0002 are shown. The solid lines denote the modified amplitude $A_{22}(t)$, and the dashed lines are the GW frequency $\omega_{22}(t)/(2\pi)$. The total mass is $M = 60M_\odot$, and the real and imaginary parts of the ringdown frequency are 300 and 40 Hz, respectively. The real frequency is obtained by multiplying by 538.609 Hz, and the real amplitude of set A is derived by dividing by 1.37903. The large difference in the inspiral phase is due to the difference of the binary parameters.

data	SNR $\rho_{\rm full}$	SNR $\rho_{\rm rd}$	injected $f_{\rm R}^{\rm (inj)}$	injected $f_{\rm I}^{\rm (inj)}$
A-01	60.0	13.81	260.68	44.58
A-02	60.0	12.73	345.16	50.49
A-03	60.0	13.79	382.53	32.58
A-04	60.0	11.84	284.18	44.73
A-05	60.0	16.78	346.20	23.07
A-06	30.0	5.57	272.85	33.40
A-07	30.0	6.56	272.85	44.54
A-08	30.0	7.27	301.89	42.24
A-09	30.0	6.93	324.60	27.25
A-10	30.0	7.88	282.55	37.45
A-11	20.0	6.36	314.24	30.58
A-12	20.0	3.45	382.10	48.60
A-13	20.0	4.68	249.36	47.97
A-14	20.0	4.13	299.32	41.88
A-15	20.0	4.54	319.42	31.55
B-01	60.0	17.58	352.56	36.20
B-02	60.0	14.27	210.78	42.77
B-03	60.0	13.67	258.83	48.42
B-04	60.0	20.09	271.13	25.40
B-05	60.0	17.07	291.99	34.20
B-06	30.0	9.53	411.57	29.48
B-07	30.0	6.29	295.78	59.38
B-08	30.0	6.03	312.39	59.24
B-09	30.0	6.01	198.34	57.91
B-10	30.0	8.31	323.32	37.86
B-11	20.0	5.20	208.80	39.75
B-12	20.0	6.60	246.66	27.85
B-13	20.0	4.46	323.71	62.51
B-14	20.0	6.20	215.15	33.15
B-15	20.0	5.85	335.20	25.11

Comparison

Comparison

TABLE III. We show the values of $\overline{\delta \log f_{\rm R}}$, $\sigma(f_{\rm R})$, $\overline{\delta \log f_{\rm I}}$, and $\sigma(f_{\rm I})$ for various methods. The results limited to set A are given on the first law of each method, while those limited to set B are on the second.

		$\overline{\delta \log f_{\rm R}}(\%)$	$\sigma(f_{\rm R})(\%)$	$\overline{\delta \log f_{\rm I}}(\%)$	$\sigma(f_{\rm I})(\%)$
MF-R	A	−12.88	28.36	−71.51	97.79
	B	−0.82	27.53	−46.11	75.48
MF-MR	A	6.25 (Very good)	17.27 (Good)	−12.62 (Very good)	37.9 (Very good)
	B	2.47	10.41	7.18	27.61
HHT	A	−13.38	21.91	−44.11	61.58
	B	−8.08	19.81	−28.78	49.61
AR	A	0.2 (Excellent)	9.93 (Excellent)	4.88 (Excellent)	38.75 (Good)
	B	1.91	8.57	6.2	34.64
NN	A	−6.64 (Good)	16.48 (Very good)	−15.23 (Good)	33.96 (Excellent)
	B	−6.65	11.97	9.96	23.76

Comparison (errors of each 60-dataset in the order of the error)

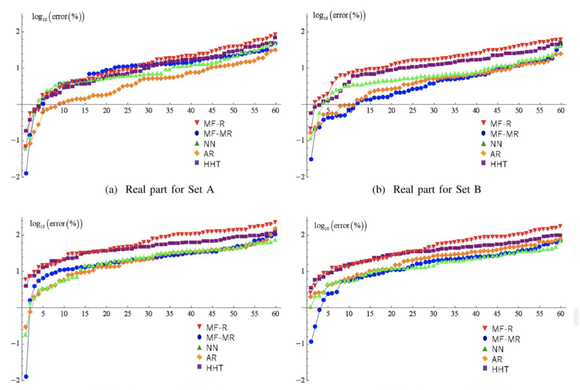

(a) Real part for Set A (b) Real part for Set B
(c) Imaginary part for Set A (d) Imaginary part for Set B

FIG. 2. Plots of the base 10 logarithm of the error in the estimate for all test data [(a) and (b) for the real part for sets A and B, respectively, and (c) and (d) for the imaginary part for sets A and B, respectively]. The data number is sorted for each method in ascending order of the magnitude of the error.

Comparison (RMS errors for low/middle/high SNR mockdata)

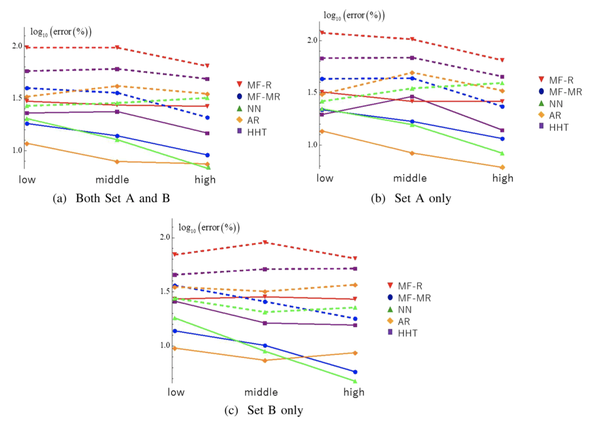

(a) Both Set A and B (b) Set A only
(c) Set B only

FIG. 3. The root-mean-square error in percent of each method for three levels of SNR [(a) for both sets A and B, (b) for only set A, and (c) for only set B]. The solid and dashed lines represent the real and imaginary parts, respectively.

Application to O1-O2 events is on-going.

Methods

method 1 :: Matched Filtering

$$(h_1|h_2) = 2\int_0^\infty \frac{\tilde{h}_1^*(f)\tilde{h}_2(f) + \tilde{h}_1(f)\tilde{h}_2^*(f)}{S_n(f)}df$$

template: $\tilde{h}_1^*(f)\tilde{h}_2(f) + \tilde{h}_1(f)\tilde{h}_2^*(f)$ — data: $\tilde{h}_2(f)$ — noise spectral density: $S_n(f)$

(a) Matched Filtering (ringdown only)

template:

$$\hat{h}(t) = \begin{cases} 0 & (t < t_0) \\ \frac{1}{N} e^{-\omega_{\rm I}(t-t_0)/Q}\cos[\omega_{\rm R}(t-t_0) - \phi_0] & (t \geq t_0) \end{cases}$$

(b) Matched Filtering (merger + ringdown)

smoothly connected templates
introducing two more parameters:
relative amplitude of ringdown vs inspiral/merger
transition rapidity of ringdown from merger

should have best performance for set B

method 2 :: Hilbert-Huang transformation (HHT)

Empirical Mode decomposition

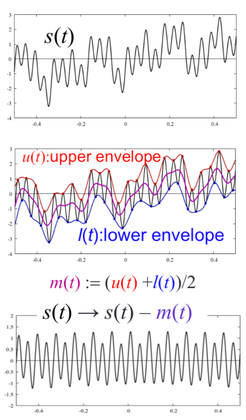

We drop high and low frequency modes by filtering the data $[f_L, f_H]$

Hilbert-Spectral Analysis

$$v(t) = \frac{1}{\pi} P\int_\infty^\infty \frac{s(\tau)}{t-\tau}d\tau$$

$$a(t)e^{i\theta(t)} = s(t) + iv(t)$$

We extract f_R (from $\theta(t)$) and f_I (from $a(t)$).

The choice of initial filtering band $[f_L, f_H]$ is a little ad hoc.

method 3 :: Auto-Regressive method (AR)

Fitting data with linear func.

$$x_n = a_1 x_{n-1} + a_2 x_{n-2} + \cdots + a_M x_{n-M} + \varepsilon = \sum_{j=1}^M a_j x_{n-j} + \varepsilon$$

- find a_j (Burg method)
- find M (FPE final prediction error method)
- re-construct wave signal from fitted function
- apply FFT with arbitrary precision.

power spectrum

$$p(f) = \frac{\sigma^2}{\left|1 - \sum_{j=1}^M a_j e^{-I2\pi j f \Delta t}\right|^2}$$

characteristic eq.

$$f(z) = 1 - \sum_{j=1}^M a_j z^j = 0$$

$|z_k|$ says amplitude,
$\arg(z_k)$ says frequency.

method 4 :: Neural Network method (NN)

Convolutional layer

$$z'_{i,l'} = \sum_{l=1}^{L}\sum_{p=1}^{H} z_{i+p,l} h^l_{p,l'} + b_{i,l'}$$

Pooling layer

$$z'_i = \max_{k=1,\ldots,p} z_{si+k}$$

Rectified linear unit (ReLU)

$$z' = h(z) = \max(z, 0)$$

Dense layer

$$z'_i = \sum_{j=1}^N w_{ij} z_j + b_i$$

layer	dimension
Input	(256, 2)
Conv	(256, 64)
Pooling	(128, 64)
ReLU	(128, 64)
Conv	(128, 128)
Pooling	(64, 128)
ReLU	(64, 128)
Conv	(64, 256)
Pooling	(32, 256)
ReLU	(32, 256)
Conv	(32, 512)
ReLU	(32, 512)
Flatten	32×512
Dense	256
ReLU	256
Dense	2
Output	2

size x channels

Choose the coefficients h, w and b to minimize loss function

$$J(y,t) = \frac{1}{M}\sum_{m=1}^M (y_m - t_m)^2$$

ACKNOWLEDGMENTS

This research made use of data generated by the Simulating eXtreme Spacetimes. This work was supported by JSPS KAKENHI Grant No. JP17H06358 (and also JP17H06357), A01: Testing gravity theories using gravi- tational waves, as a part of the innovative research area, "Gravitational wave physics and astronomy: Genesis" . H. N. acknowledges support from JSPS KAKENHI Grant No. JP16K05347. The work of T. N. was also supported in part by a Grant-in-Aid for JSPS Research Fellows. H. S. acknowledges also support from JSPS KAKENHI Grants No. JP18K03630 and No. 19H01901. H. T. acknowledges support from JSPS KAKENHI Grant No. JP17K05437. T. T. acknowledges support from JSPS KAKENHI Grants No. JP26287044 and No. JP15H02087.